Biochemistry

Article

Cite This: *Biochemistry* 2019, 58, 3293−3301

pubs.acs.org/biochemistry

Mo-, V-, and Fe-Nitrogenases Use a Universal Eight-Electron Reductive-Elimination Mechanism To Achieve N_2 Reduction

Derek F. Harris,[†] Dmitriy A. Lukoyanov,[‡] Hayden Kallas,[†] Christian Trncik,[§] Zhi-Yong Yang,[†] Phil Compton,[‡] Neil Kelleher,[‡] Oliver Einsle,[§] Dennis R. Dean,[∥] Brian M. Hoffman,*[,‡] and Lance C. Seefeldt*[,†]

[†]Department of Chemistry and Biochemistry, Utah State University, Logan, Utah 84322, United States

[‡]Department of Chemistry, Northwestern University, Evanston, Illinois 60208, United States

[§]Institut für Biochemie, Albert-Ludwigs-Universität Freiburg, 79104 Freiburg, Germany

[∥]Department of Biochemistry, Virginia Polytechnic Institute and State University, Blacksburg, Virginia 24061, United States

Supporting Information

ABSTRACT: Three genetically distinct, but structurally similar, isozymes of nitrogenase catalyze biological N_2 reduction to $2NH_3$: Mo-, V-, and Fe-nitrogenase, named respectively for the metal (*M*) in their active site metallocofactors (metal-ion composition, MFe_7). Studies of the Mo-enzyme have revealed key aspects of its mechanism for N_2 binding and reduction. Central to this mechanism is accumulation of four electrons and protons on its active site metallocofactor, called FeMo-co, as metal bound hydrides to generate the key $E_4(4H)$ ("Janus") state. N_2 binding/reduction in this state is coupled to reductive elimination (*re*) of the two hydrides as H_2, the forward direction of a reductive-elimination/oxidative-addition (*re/oa*) equilibrium. A recent study demonstrated that Fe-nitrogenase follows the same *re/oa* mechanism, as particularly evidenced by HD formation during turnover under N_2/D_2. Kinetic analysis revealed that Mo- and Fe-nitrogenases show similar rate constants for hydrogenase-like H_2 formation by hydride protonolysis (k_{HP}) but significant differences in the rate constant for H_2 *re* with N_2 binding/reduction (k_{re}). We now report that V-nitrogenase also exhibits HD formation during N_2/D_2 turnover (and H_2 inhibition of N_2 reduction), thereby establishing the *re/oa* equilibrium as a universal mechanism for N_2 binding and activation among the three nitrogenases. Kinetic analysis further reveals that differences in catalytic efficiencies do not stem from significant differences in the rate constant (k_{HP}) for H_2 production by the hydrogenase-like side reaction but directly arise from the differences in the rate constant (k_{re}) for the *re* of H_2 coupled to N_2 binding/reduction, which decreases in the order Mo > V > Fe.

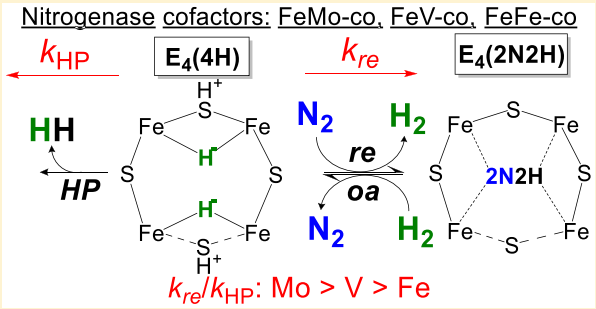

Nitrogenases are microbial enzymes that reduce dinitrogen (N_2) to ammonia (NH_3) as part of the global nitrogen cycle.[1−3] The nitrogenase family consists of three known isozymes, Mo-nitrogenase, V-nitrogenase, and Fe-nitrogenase, with each form encoded by unique gene clusters: Mo-nitrogenase by *nif*, V-nitrogenase by *vnf*, and Fe-nitrogenase by *anf*.[4−9] They are all two-component systems. The Fe protein components, designated NifH, VnfH, and AnfH, are agents of electron delivery to the catalytic components, designated MoFe protein (NifDK), VFe protein (VnfDGK), or FeFe protein (AnfDGK). The catalytic components house the sites for substrate binding and reduction, which are complex, structurally similar metallocofactors denoted FeMo-cofactor (FeMo-co), FeV-cofactor (FeV-co), or FeFe-cofactor (FeFe-co), with structural representations of these cofactors shown in Figure 1.[4,5,8−17]

Our understanding of the nitrogenase mechanism primarily comes from studies with the Mo-nitrogenase, which is the most widespread and largest contributor to the nitrogen cycle and therefore the best studied of the three forms. Substrate reduction by Mo-nitrogenase involves electron delivery to MoFe protein by the Fe protein, which transfers one electron during association of the two components, followed by hydrolysis of two ATP molecules bound to the Fe protein to initiate their dissociation.[5,10,18−21] The stepwise process of electron and proton accumulation by the cofactor can be visualized as shown in Figure 2A, which is a simplified version of the kinetic scheme proposed by Lowe and Thorneley (LT)[21] and recently established by studies of trapped catalytic intermediates.[10,22−24] This scheme omits proposed reactivity at E3, which is not significant under the high flux conditions used here. N_2 binds to the cofactor after delivery of $4e^-/4H^+$ has

Received: May 28, 2019
Revised: June 27, 2019
Published: July 8, 2019

DOI: 10.1021/acs.biochem.9b00468
Biochemistry 2019, 58, 3293−3301

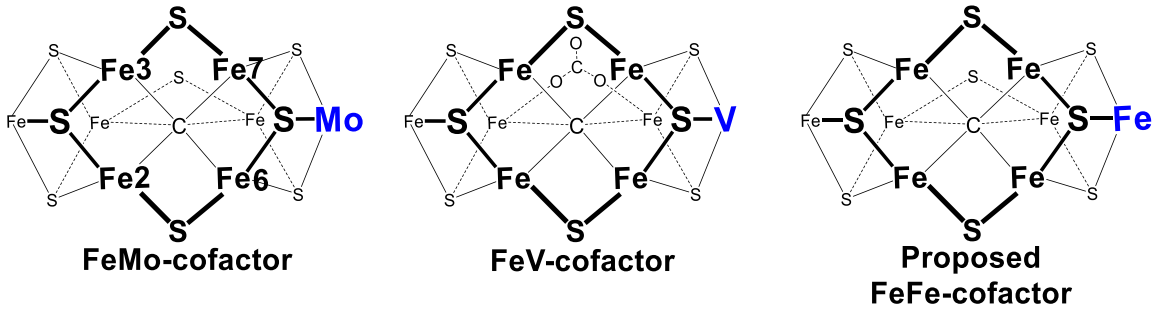

Figure 1. Nitrogenase cofactors. Structures of the FeMo-cofactor of Mo-nitrogenase, FeV-cofactor of V-nitrogenase, and proposed structure of the FeFe-cofactor of Fe-nitrogenase. View is looking down on the Fe2, 3, 6, 7 face with Fe atoms numbered. *R*-homocitrate would be to the right in each (not shown).

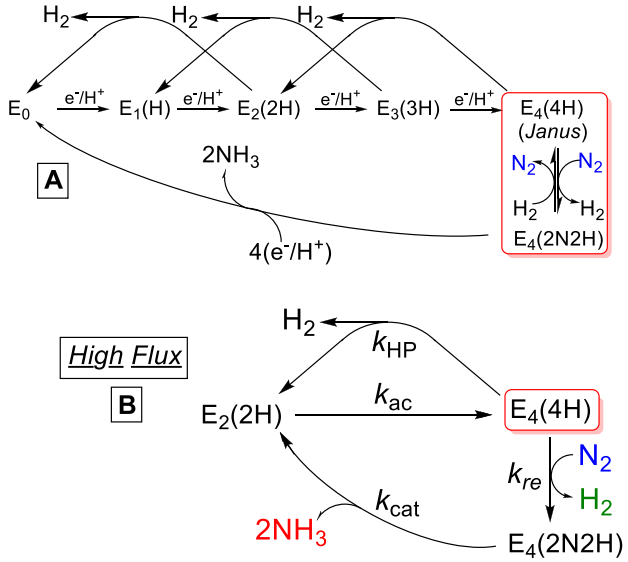

Figure 2. Kinetic schemes. (**A**) Simplified Thorneley and Lowe kinetic scheme for N_2 reduction. The "red box" highlights the key step in catalysis, the reductive-elimination/oxidative addition. This scheme maps onto (**B**) under high-flux, steady-state turnover conditions. Starting at E_4 the enzyme can either perform hydride protonolysis (HP) with rate k_{HP} resulting in the E_2 state from which E_4 is regenerated at the rate of electron accumulation k_{ac} or capture N_2 with rate k_{re} that is fully reduced to 2 NH_3 with an overall rate constant of k_{cat}. Full N_2 reduction regenerates E_0 and subsequently E_1 before E_2 is regenerated, but for the purposes of this simplified model E_0 and E_1 are not considered.

generated $E_4(4H)$, which stores them as two bridging hydrides, [Fe−H−Fe]. The two hydrides of this key intermediate can undergo reductive elimination (*re*) of H_2, and N_2 binding with displacement of H_2 leads to cleavage of the N≡N triple bond to generate the $E_4(2N2H)$ state.[10,21−26] The subsequent delivery of 4 additional electrons/protons produces 2 NH_3 products to complete the catalytic cycle. Based on their overall structural similarities to the Mo-nitrogenase, the V- and Fe-nitrogenases would seem likely to follow this same general mechanism of electron delivery and accumulation.[4,8,9,12,14−17] However, it has been reported that they differ in the amount of H_2 produced per N_2, resulting in different limiting stoichiometries for the overall reaction (eqs 1−3).[8,13,27,28]

Mo-nitrogenase:

$$N_2 + 8H^+ + 16MgATP + \mathbf{8}e^- \rightarrow 2NH_3 + \mathbf{1}H_2 + 16MgADP + 16P_i \quad (1)$$

V-nitrogenase:

$$N_2 + 12H^+ + 24MgATP + \mathbf{12}e^- \rightarrow 2NH_3 + \mathbf{3}H_2 + 24MgADP + 24P_i \quad (2)$$

Fe-nitrogenase:

$$N_2 + 20H^+ + 40MgATP + \mathbf{20}e^- \rightarrow 2NH_3 + \mathbf{7}H_2 + 40MgADP + 40P_i \quad (3)$$

Such differences in limiting H_2/N_2 stoichiometry would suggest different mechanisms of N_2 reduction by the three nitrogenases and that they differ greatly in their tendency to undergo hydride protonolysis to generate H_2 in a hydrogenase-like side reaction.

In fact, a recent study of the Fe-nitrogenase has demonstrated that this enzyme does *not* exhibit the limiting behavior of eq 3 but rather follows the *re/oa* mechanism for N_2 binding, with the stoichiometry of eq 1 established for Mo-nitrogenase.[13,29] In that report, it was suggested that the V-nitrogenase behaves similarly, following the *re/oa* mechanism, but this was *not* experimentally verified. We do so in the present study, thereby completing the demonstration that all three nitrogenases exhibit the *re/oa* mechanism for N_2 binding and activation, with the attendant limiting stoichiometry of $H_2/N_2 \rightarrow 1$ as $P_{N_2} \rightarrow \infty$. The results further provide a comparison of key kinetic parameters for the three nitrogenases, thus providing a complete picture of the differences in reactivity of the catalytically central $E_4(4H)$ intermediate among the three enzymes.

■ MATERIALS AND METHODS

Reagents and General Procedures. All reagents were obtained from Sigma-Aldrich (St. Louis, MO), Fisher Scientific (Fair Lawn, NJ), or Bio-Rad (Hercules, CA) unless specified otherwise and used without further purification. Argon and dinitrogen gases were purchased from Air Liquide America Specialty Gases LLC (Plumsteadville, PA). Manipulation of proteins and buffers was done anaerobically in septum-sealed serum vials and flasks using a vacuum Schlenk line, argon or dinitrogen atmospheres, and gastight syringes. Gas transfers were made using gastight syringes.

Bacterial Growth and Protein Purification. Fe-nitrogenase proteins (FeFe and Fe protein) were expressed and purified from *Azotobacter vinelandii* strain DJ1255 as previously described.[13] Mo-nitrogenase proteins (MoFe and Fe protein)

DOI: 10.1021/acs.biochem.9b00468
Biochemistry 2019, 58, 3293−3301

were expressed and purified from *Azotobacter vinelandii* strains DJ995 (His-MoFe protein) and DJ884 (Fe protein) as previously described.[30−32] V-nitrogenase proteins (VFe and Fe protein) were expressed and purified from *Azotobacter vinelandii* strain Lipman 1903 as previously described.[33] Additional V-nitrogenase Fe protein was expressed and purified from *Azotobacter vinelandii* strain DJ1258 by previously described methods with minor modifications, substituting 10 mM Na_3VO_4 for the Na_2MoO_4 in the growth media.[30−32] All proteins were concentrated anaerobically under an inert gas atmosphere. Protein concentrations were determined using the Bio-Rad DC Protein Assay Kit or the Biuret method. Protein purity was assessed by SDS-PAGE with Coomassie Brilliant Blue staining.

Proton and Dinitrogen Reduction Assays and Inhibition of N_2 Reduction by H_2. Substrate reduction assays were performed in 9.4 mL serum vials containing a MgATP regeneration buffer (6.7 mM $MgCl_2$, 30 mM phosphocreatine, 5 mM ATP, 0.2 mg/mL creatine phosphokinase, 1.2 mg/mL BSA) and 10 mM sodium dithionite in 100 mM MOPS buffer at pH 7.0. Reaction vials were made anaerobic, and their headspaces were adjusted to the partial pressure of N_2 gas or H_2 gas desired with the remaining headspace made up of argon. In H_2 inhibition of N_2 reduction assays N_2 gas in the headspace was held constant at 0.4 atm with H_2 gas varied. The MoFe, VFe, or FeFe protein was then added to the vials, the vials were vented to atmospheric pressure, and the reactions were initiated by the addition of the appropriate Fe protein (NifH, VnfH, or AnfH). MoFe, VFe, or FeFe concentrations in reactions were 0.1 mg/mL, corresponding to ∼0.4 nmol per reaction vial. Assays were performed at a molar ratio of 1:20 for MoFe:Fe protein, 1:20 for VFe:Fe protein, and 1:30 for FeFe:Fe protein, except in a series of measurements designed to test the specific activity as a function of the electron flux, which is controlled by this ratio. Reactions were conducted at 30 °C for 8 min and then stopped by the addition of 300 μL of 400 mM EDTA (pH 8.0). The flux dependence of N_2 reduction by Mo-nitrogenase employed a buffer containing a MgATP regeneration system (5 mM $MgCl_2$, 22 mM phosphocreatine, 3.8 mM ATP, 0.15 mg/mL creatine phosphokinase, 0.8 mg/mL BSA) with 0.125 mM 1,4-dithiothreitol, 0.6 mM flavodoxin in the hydroquinone state (Fld^{HQ}), and 12 mM sodium dithionite in 100 mM MOPS at pH 7.3. The Fe protein concentration was fixed at 0.1 mg/mL, and the MoFe protein concentration was varied from 0.2 to 6.4 mg/mL to give a ratio of [MoFe]/[Fe] from 0.5 to 16. The reactions were incubated at 30 °C for 30 s under 1 atm of N_2 and then stopped by the addition of 500 μL of 400 mM EDTA (pH 8.0). H_2 and NH_3 were quantitated according to published methods.[34,35]

Kinetics Analysis. Kinetics equations were modeled in Mathcad 15 or QtiPlot v5.6.1 and fit to experimental data using the latter.

HD Production. Turnover samples were prepared, initiated, and terminated as described above with the exception that they were turned over for 15 min. Paired control samples with proteins excluded and the liquid volume contribution from the proteins substituted with EDTA were prepared and handled identically to the turnover samples to establish HD contamination levels in the D_2 gas. The D_2 gas in the headspace was held constant at 0.3 atm with N_2 gas varied. In turnover samples, VFe protein was used at 0.2 mg/mL and Fe protein was used at 0.38 mg/mL for a VFe:Fe protein molar ratio of 1:7.5.

Volumes of HD produced by V-nitrogenase during reaction in the vials were measured with Inficon L100 RGA as previously described; note that the capillary was 30 μm i.d.[13] The mass-to-charge ratio (m/z) of 3 for HD was used. No-turnover blank samples prepared without proteins but with the same volume of solvent and the same gas mixture as turnover samples were tested for the background level induced by HD contamination of the D_2 gas. The headspace of each sample vial was tested for the m/z = 3 responses multiple times, and the measured levels were higher for VFe turnover samples than for no-turnover samples of the same N_2/D_2 ratio mixture. The difference levels after background subtraction were assigned to HD produced during reaction and converted into volume units with previously obtained calibration.[13] Comparison of m/z = 3 and 4 signals acquired for no-turnover samples gave an estimate of 0.18 ± 0.03% for HD contamination of the D_2 gas (note: in the previous similar study of FeFe nitrogenase the contamination was determined as 0.15 ± 0.02%).

RESULTS

Kinetic Analysis. The critical step in the *re/oa* mechanism that has been shown to characterize both the Mo- and Fe-nitrogenases is the *re* of the two bridging hydrides of the $E_4(4H)$ Janus intermediate to generate H_2, with release of H_2 upon binding of N_2 and cleavage of the N≡N triple bond (Figure 3).[5,10,13,22−25,36] However, this reaction at $E_4(4H)$

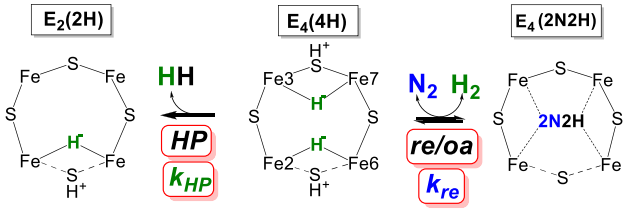

Figure 3. Reactions of the E_4 state. The $E_4(4H)$ state (middle) is shown reacting to the left by hydride protonolysis (HP) to generate $E_2(2H)$ with H_2 production, rate constant k_{HP}, or undergoing *re* (reductive elimination) and to the right, loss of H_2 upon binding/reaction of N_2, rate constant k_{re}. The hydride and proton positions represent the structure populated at cryogenic temperatures and the lowest energy structure in DFT computations.[25] The computations show a number of nearly isoenergetic isomers that are likely accessible at room temperature. The possible hemilability of an S is noted with dotted lines; "2N2H" denotes a diazene-level intermediate of undetermined structure.

occurs in competition with the hydride protonolysis (HP) reaction to generate H_2 without N_2 binding, as shown in Figures 2A and 3.[21,29] As a result, under most conditions of electron-delivery "flux" and partial pressure of N_2 (P_{N_2}), the ratio of H_2 produced to N_2 reduced, $r = H_2/N_2 > 1$. To achieve the limiting stoichiometry of eq 1 requires not only high P_{N_2} as evidenced by Simpson and Burris[27] but also high electron flux, characterized by a high [Fe]/[*M*Fe] ratio, with a resulting rate of electron delivery during electron accumulation (rate constant k_{ac} in Figure 2, Scheme B) much greater than that for the competing H_2 production by HP (rate constant k_{HP}) at states E_n, n = 2, 3 in Scheme A.[29] Under these high flux conditions, catalytic behavior can be represented as shown in Figure 2, Scheme B, in which H_2 production at electron-

DOI: 10.1021/acs.biochem.9b00468
Biochemistry 2019, 58, 3293−3301

accumulation stages, E_n, $n \leq 3$, is suppressed during turnover as these states become depopulated in favor of the E_4-level states, and *all* reaction occurs at $E_4(4H)$. Thus, high-flux, steady-state experiments (Figure 2, Scheme B) are of particular importance in that they emphasize the role of $E_4(4H)$ as the "Janus intermediate", a catalytic "branch point" that can react in one of two ways. It can "fall back" in a hydrogenase-like catalytic cycle, releasing H_2 by the first-order HP process (rate constant k_{HP}) without further electron accumulation, or it can be "captured" by a second-order reaction with N_2 (rate constant k_{re}) with accompanying release of H_2 formed by *re*, to produce $E_4(2N2H)$ (Figure 3), which irreversibly carries on to generate $2NH_3$ with a composite rate constant, k_{cat}.[29] Of central significance in steady-state turnover experiments described by Scheme B, k_{ac} and k_{cat} are composite rate constants, while the rate constants k_{HP} and k_{re} correspond precisely to the rate constants for reaction of $E_4(4H)$ in Scheme A and indeed in the full LT scheme. High-flux experiments thus provide precision measurements of the centrally important mechanistic rate constants that define the $E_4(4H)$ branch point: k_{HP} and k_{re}.[29]

As previously shown, during steady-state turnover the differential equations for the rates of formation of H_2 and NH_3 and loss of N_2 are zero-order in time, and the total formation of $2NH_3$/loss of N_2 and the formation of H_2 during a turnover experiment are simply proportional to their respective steady-state rate constants (eq 4), where E_0^0 is the total enzyme concentration.[29]

$$\frac{dNH_3}{dt} = -2\frac{dN_2}{dt} \overset{SS}{\rightarrow} k_{NH_3}\cdot E_0^0 \qquad \frac{dH_2}{dt} \overset{SS}{\rightarrow} k_{H_2}\cdot E_0^0 \tag{4}$$

The rate constant for NH_3 formation per electron is given by eq 5; the bracketed term in the second form of eq 5 has the form of a binding isotherm, with the flux-dependent apparent binding constant, K_a^z. The dependence of NH_3 production is here written as a function of the ratio of rate constants for electron delivery and HP, $z = k_{ac}/k_{HP}$, which increases with an increasing ratio of nitrogenase component protein concentrations

$$k_{NH3} = 2k_{N2} \overset{SS}{\rightarrow} \left(\frac{1}{4}\right)\frac{(k_{re}P_{N2})}{\left(1+\frac{1}{z}\right)+\frac{(k_{re}P_{N2})}{\bar{k}}} = \left(\frac{1}{4}\right)\bar{k}\left[\frac{K_a^z P_{N2}}{1+K_a^z P_{N2}}\right] \tag{5}$$

$$z = \frac{k_{ac}}{k_{HP}} = b\bullet\frac{[Fe]}{[MFe]} \qquad \bar{k} = \frac{k_{ac}k_{cat}}{k_{ac}+k_{cat}} \qquad K_a^z = \frac{k_{re}z}{(1+z)\bar{k}}$$

where z is defined as the inverse of the definition in our earlier report.[29] This is a more natural formulation: z as defined in eq 5 now increases with flux, as the efficacy of electron delivery from Fe protein > *M*Fe protein increases. The corresponding rate constant for H_2 production for Scheme B is presented in eq S1.

Scheme B and the resultant steady-state turnover rate constants provide a clear mathematical formulation of the competition at the $E_4(4H)$ branch point between the first-order process of H_2 formation by HP without N_2 binding and the second-order *re* process in which the binding and reduction of one N_2 accompany the *re* of one H_2. This ability of a second-order process to out-compete a first-order one is most clearly captured by taking the ratio of the rate constants for production of H_2 (eq S1) and N_2 consumption (eq 5) denoted r, which can be written, in terms of the rate-constant ratio for the two processes, ρ, as eq 6. See ref 29 for further discussion of the equations describing Scheme B.

$$r = \frac{k_{H2}}{k_{N2}} = \left[\frac{1+\left(\frac{1}{4}\right)\left(1+\frac{4}{z}\right)\rho P_{N2}}{\left(\frac{1}{4}\right)\bullet\rho P_{N2}}\right] \qquad \rho = \left(\frac{k_{re}}{k_{HP}}\right) \tag{6}$$

Kinetic Measurements. When Mo-nitrogenase is turning over under 1 atm of N_2 at high electron flux (20 Fe protein to 1 MoFe protein), the ratio of H_2 formed to N_2 consumed is ~2 (Figure 4). As the electron flux through nitrogenase decreases,

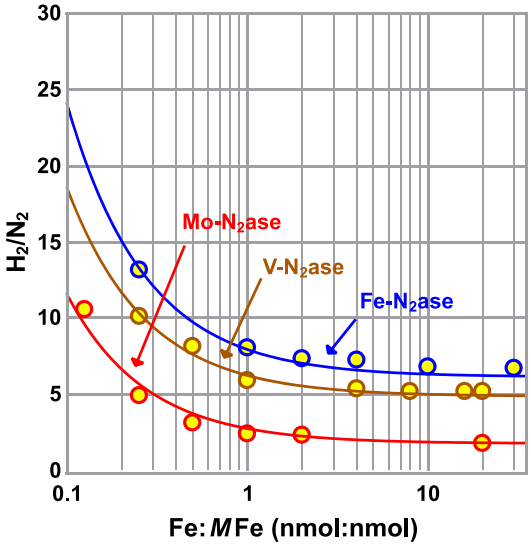

Figure 4. Ratio of H_2 formed to N_2 reduced as a function of flux under 1 atm N_2, which is proportional to the ratio of Fe protein to *M*Fe protein (where *M* = Mo, V, or Fe) for all three forms of nitrogenase (Mo-nitrogenase in red, V-nitrogenase in brown, and Fe-nitrogenase in blue). Traces were calculated by fixing ρ as determined below (Table 1) and fitting the parameter b in eq 6. One data set is shown, which is representative of two data sets. Fit parameters were the same for the two data sets. Assays were performed as described in Materials and Methods.

by lowering the ratio Fe protein to MoFe protein, the ratio of H_2 formed per N_2 consumed increases. These data, and the corresponding measurements for Fe- and V-nitrogenases, can be fit to eq 6 that describes the relationship between the H_2/N_2 ratio and the flux parameter, z, defined in eq 5 as a ratio of Fe protein to MFe protein (Fe:*M*Fe) with a proportionality constant, b, which relates the flux and protein ratio. Values of b for the three nitrogenases obtained by fitting the data are listed in Table 1. Note that because the value is different for the three enzymes, care must be taken when comparing activities at a fixed ratio, [Fe]/[*M*Fe], unless in the high-flux limit.

As seen earlier, Fe-nitrogenase shows the same general trend of decreasing H_2/N_2 as the electron flux increases (Figure 4), with a notable difference from Mo-nitrogenase that the ratio of H_2 formed to N_2 reduced at P_{N_2} = 1 atm is higher at every flux and approaches just a ratio of ~7 at high electron flux.[29] Both Mo- and Fe-nitrogenase show a sharp decrease in the H_2/N_2

DOI: 10.1021/acs.biochem.9b00468
Biochemistry 2019, 58, 3293−3301

Table 1. Kinetic Parameters Obtained from High-Flux Turnover (Fe/*M*Fe) ≥ 20

M	$\rho = k_{re}/k_{HP}$ $(atm^{-1})^b$	k_{re} $(s^{-1}atm^{-1})^c$	$K_a = k_{re}/\bar{k}$ $(atm^{-1})^a$	k_{HP} $(s^{-1})^c$	$\bar{k}$ $(s^{-1})^a$	b^d
Mo	5.1(1)	83.5	7.3(3)	16.4	11.3	4.1(2)
V	1.1(1)	24.2	2.7(3)	22	8.8	2.9(4)
Fe	0.78(3)	8.4	1.8(1)	10.8	4.6	2.2(1)

[a]Obtained from fits of data in Figure 5 to eq 5. [b]Obtained from fits of data in Figure 6 to eq 6 allowing z to be large. Standard errors from three measurements are shown in parentheses. [c]Calculated from other parameters using definitions in eqs 5 and 6. [d]Obtained from fits in Figure 4 using eq 6 with ρ fixed to the value shown in the table.

ratio as flux increases to approximately 1 Fe protein to 1 MoFe protein. Above this ratio (higher flux), the H_2 to N_2 ratio remains constant, indicative of the transition to the "high-flux" regime. Figure 4 also shows the H_2/N_2 ratio for V-nitrogenase as a function of electron flux (Fe:VFe), which was not previously reported. As can be seen, V-nitrogenase behaves similarly to the Mo- and Fe-nitrogenases, transitioning to the high-flux regime at a Fe:*M*Fe ratio of ~1, but with the ratio of H_2/N_2 at P_{N_2} = 1 atm falling between the values for Mo- and Fe-nitrogenases for every value of the flux.

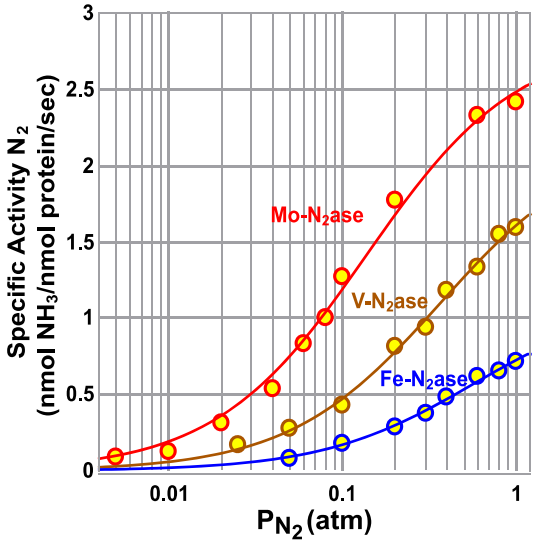

Figure 5. Specific activities for N_2 reduction by all three forms of nitrogenase as a function of partial pressure of N_2 at high flux (Fe/*M*Fe) ≥ 20 (Mo-nitrogenase in red, V-nitrogenase in brown, and Fe-nitrogenase in blue). Overlaid are fits to eq 5 obtained with QtiPlot; values for $\bar{k}$ and K_a^z for each are listed in Table 1. One data set is shown, which is representative of two data sets. Fit parameters were the same for the two data sets. Assays were performed as described in Materials and Methods.

Figure 5 shows the specific activities for N_2 reduction as a function of partial pressure of N_2 (P_{N_2}) for all three nitrogenases. The P_{N_2} dependence for each is well fit by eq 5, which provides values for the apparent binding constant, which at the high flux values $z \rightarrow \infty$ approaches the limiting form, $K_a = k_{re}/\bar{k}$, the ratio of rate constants for N_2 capture, generating $E_4(2N2H)$ (k_{re}), and apparent velocity parameter ($\bar{k}$), with the resulting measured and calculated values for the three nitrogenases listed in Table 1. The k_{re} for N_2 of V-nitrogenase is intermediate between that for Mo- and Fe-nitrogenases, being ~3.5 times lower than the value for Mo-nitrogenase and ~3 times higher than the value for the Fe-nitrogenase. On the other hand, K_a for V-nitrogenase is only ~1.5 times greater than that for Fe-nitrogenase but is ~3 times less than for Mo-nitrogenase. Interestingly, $\bar{k}$ for V-nitrogenase is very similar to that for Mo-nitrogenase, while $\bar{k}$ for Fe-nitrogenase is at least 50% less than for Mo- and V-nitrogenases.

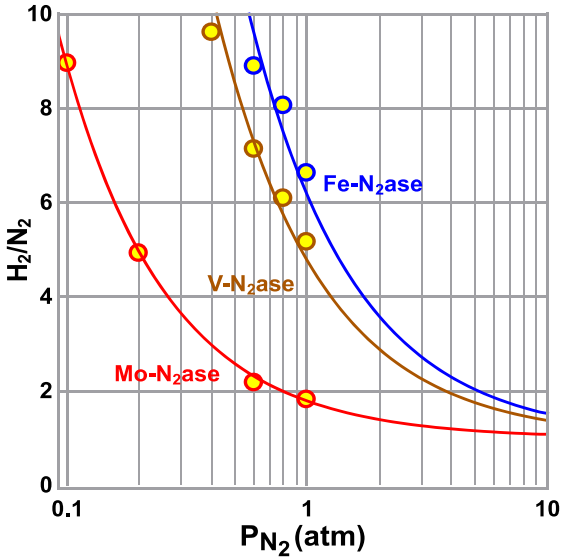

Figure 6. Ratio of H_2 formed to N_2 reduced as a function of partial pressure of N_2 for all three forms of nitrogenase at high flux (Fe/*M*Fe) ≥ 20 (Mo-nitrogenase in red, V-nitrogenase in brown, and Fe-nitrogenase in blue). Overlaid are fits to eq 6 obtained with QtiPlot. Measured values for $\rho = (k_{re}/k_{HP})$ are listed in Table 1. One data set is shown, which is representative of two data sets. Fit parameters were the same for the two data sets. All assays were performed as described in Materials and Methods.

Figure 6 presents the high-flux H_2/N_2 ratio as a function of P_{N_2}. The measurements for all three forms are well-described by the expression of eq 6 as derived from Scheme B. The single parameter, $\rho = k_{re}/k_{HP}$, that controls this expression precisely captures the competition between the productive (rate-constant, k_{re}) and nonproductive (k_{HP}) reactions of the $E_4(4H)$ Janus intermediate illustrated in Figure 3. The value of ρ for the V-nitrogenase is quite comparable to that for Fe-nitrogenase, with the two being ~5-fold less than ρ of Mo-nitrogenase. By combining the parameters obtained from the fits of the specific activities (Figure 5) and H_2/N_2 ratios (Figure 6) to eqs 5 and 6, respectively, one obtains the individual rate constants k_{HP} and k_{re} for the three nitrogenases, Table 1. Comparison reveals that k_{HP} is less that a factor of 2 larger for the two alternative nitrogenases compared to the Mo variant, whereas k_{re} for V-nitrogenase is 3-fold smaller than for the Mo form, and that for Fe-nitrogenase is 10-fold smaller.

H_2 Inhibition of N_2 Reduction in V-Nitrogenase. A mechanistically important feature of the Mo- and Fe-nitrogenases is the inhibition of N_2 reduction by H_2.[5,10,13,36] This can be understood as arising because H_2 acts through the

DOI: 10.1021/acs.biochem.9b00468
Biochemistry 2019, 58, 3293−3301

re/oa equilibrium (Figure 2A), to disfavor N_2 binding/reduction and ultimately NH_3 formation. Figure 7 shows that

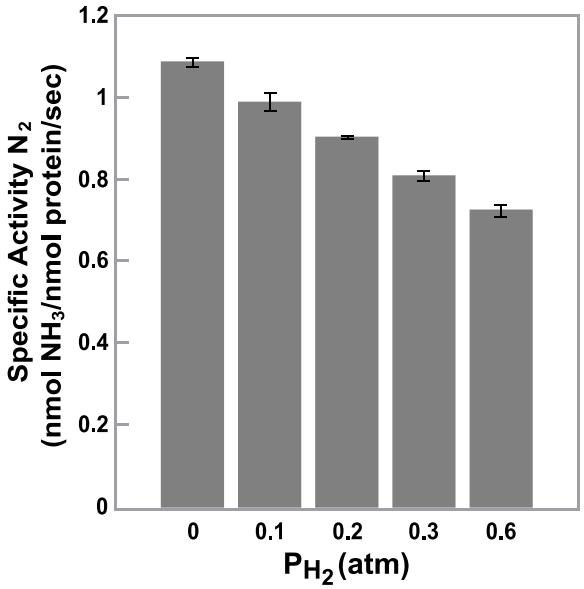

Figure 7. H_2 inhibition of N_2 reduction for V-nitrogenase: specific activity for NH_3 production as a function of P_{H_2} for P_{N_2} = 0.4 atm. Data are the average of two independent experiments (with error bars), performed as described in Materials and Methods.

at high flux, when P_{N_2} is held constant at 0.4 atm, which is close to the measured K_M ($K_M = 1/K_a$ = 0.37 atm), as the partial pressure of H_2 is increased the specific activity for N_2 reduction decreases, showing ~35% inhibition at an H_2/N_2 ratio of 0.6 atm/0.4 atm, as expected for the *re/oa* mechanism (Figure 3).

HD Formation. The most compelling test of the *re/oa* mechanism is to carry out N_2 inhibition under a partial pressure of D_2, rather than H_2. In the absence of N_2, D_2 completely fails to react with nitrogenase, but in the presence of N_2, D_2 is consumed, stoichiometrically forming two HD.[5,10,36,37] This observation is explained by the *re/oa* mechanism. D_2 reacts with E_4(2N2H) and undergoes *oa* to form E_4(2H2D), which contains two bridging D^-; all other exchangeable sites contain protons from the H_2O buffer. Hydrogenase-like protonolysis of those deuterides (DP) produces the observed two HD (see Figure S1). The HD formation is thus a signature of the *re/oa* mechanism, which was long-known for Mo-nitrogenase, and we recently showed it to occur for Fe-nitrogenase.[5,10,13,36,37]

The V-nitrogenase was thus tested for HD formation in the presence N_2 and D_2. In these experiments, the partial pressure of D_2 (P_{D_2}) was held constant at 0.3 atm, and the partial pressure of N_2 was varied (Figure 8). The HD was quantitated after turnover for a fixed time by mass spectrometric analysis of the gas phase. As can be seen, HD is indeed produced by V-nitrogenase, and the amount increases with increasing P_{N_2} at a fixed partial pressure of D_2. Both observations are as expected from consideration of the *re/oa* equilibrium (Figures 2 and 3), in which the concentration of E_4(2N2H) increases with P_{N_2}; the rate of *oa* reaction of D_2 to generate E_4(2H2D) is proportional to P_{D_2} and the concentration of E_4(2N2H). Subsequent relaxation of E_4(2H2D) generates a single

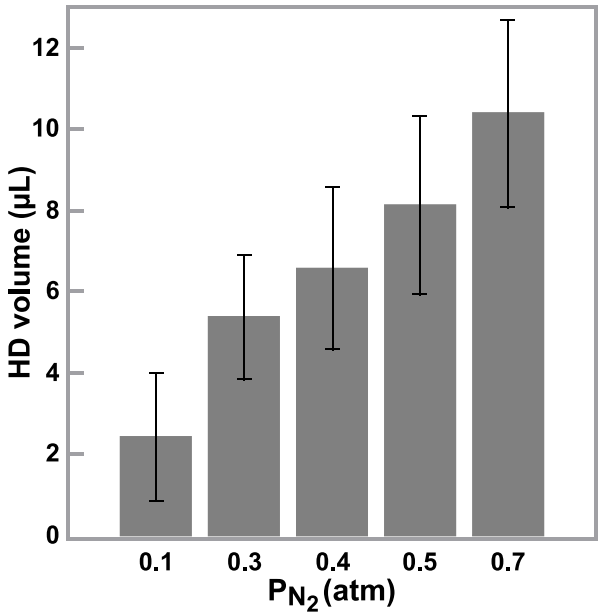

Figure 8. HD formation by V-nitrogenase. Volume of produced HD in the turnover sample vials as a function of P_{N_2} with P_{D_2} fixed at 0.3 atm. Error bars represent standard deviations for two independent assays performed as described in Materials and Methods.

molecule of HD and an intermediate, E_2(HD), that in turn can relax to E_0 through generation of a second HD.

DISCUSSION

The majority of studies aimed at understanding the kinetics and mechanism of N_2 reduction by nitrogenase has focused on the Mo-nitrogenase.[5,10,21,38] These studies have marked significant progress, producing kinetic schemes for Fe protein and MoFe protein cycles,[21,39−42] multiple solved structures,[17,43−49] and an understanding of the steps leading to, and mechanism of, N_2 binding.[10,22−26] Such studies were recently extended to the alternative Fe-nitrogenase,[8,13,29] but the prior work on the V-nitrogenase[9,50−52] was not similarly extended. Structural studies have shown that the multimetallic FeV-co of V-nitrogenase[14,53] has a quite similar structure to that of FeMo-co, and a corresponding similarity is presumed for FeFe-co.[12] However, despite overall structural similarities, the different nitrogenases appeared to show fundamental differences in reactivity toward N_2 and protons.[8,13,27,28] Most significantly, the accepted view that they each exhibit a different limiting stoichiometry of H_2 produced for each N_2 reduced, eqs 1−3, implied that each has a different mechanism for N_2 reduction. The present report instead completes the determination that the three forms each function through a common *re/oa* mechanism, as originally established for Mo-nitrogenase.

Mechanism of N_2 Binding and Activation. The first indicator of mechanism for the nitrogenases is inhibition of N_2 reduction by the presence of H_2 (Figure 7), which is explained by the *re/oa* mechanism, Figure 3. Such inhibition is well-known for Mo-nitrogenase, was recently shown for the Fe-nitrogenase, and is here reported for the V-nitrogenase.[5,13,21] However, the gold standard for establishing reversibility of the E_4(4H) ⇔ E_4(2N2H) couple is the formation of HD when the enzyme is turned over in the presence of D_2 and N_2, as a

DOI: 10.1021/acs.biochem.9b00468
Biochemistry 2019, 58, 3293−3301

consequence of the *re/oa* mechanism.[5,10,13,36,37] As can be seen in Figure 8, V-nitrogenase shows HD formation that increases with increasing P_{N_2}, as a result of increases in the population of $E_4(2N2H)$ with P_{N_2}. When normalized for protein concentration, the HD produced by V-nitrogenase is twice that previously seen with the Fe-nitrogenase, which is in agreement with the ∼2-fold greater specific activity for N_2 reduction of V-nitrogenase over Fe-nitrogenase per P_{N_2} (Figure 5).[13] This observation that V-nitrogenase also follows a *re/oa* mechanism shows that all three nitrogenases follow a universal mechanism for N_2 reduction: the *re/oa* equilibrium activation process of Figures 2 and 3.

Kinetic Analysis. An understanding of the source of the differences in reactivity among the three nitrogenases comes from the careful kinetic analysis of the relative reactivities for N_2 and proton reduction as a function of the partial pressure of N_2 under different electron flux conditions (ratio of Fe protein to the catalytic component). The steady-state kinetic model recently applied to Mo- and Fe-nitrogenases, and here applied systematically to all three enzymes, provides an understanding of the similarities and differences of the three nitrogenases that is inaccessible to pre-steady state kinetic approaches.[29]

First, the three enzymes differ only modestly in their ability to accumulate electrons, with the flux parameter, $z = b[Fe]/[MFe]$, characterized by a proportionality constant, b, varying for the three in the ratio Mo/V/Fe ∼ 4/3/2 (Table 1), and with all three transitioning to the high-flux limit of electron accumulation by, or slightly above, the component ratio, $[Fe]/[MFe] \sim 1$, Figure 4.

Monitoring the ratio, $r = H_2/N_2$ under the high-flux limit in the steady-state as a function of P_{N_2} reveals how the differences in catalytic effectiveness of the three nitrogenases arise from the difference in the reactivity of their $E_4(4H)$ states. The parameter ρ produced through fits of the data in Figure 6 to eq 6 is the ratio of the key rate constants for the competing reactions of the central $E_4(4H)$ state, k_{re}/k_{HP}. This ratio captures the relative tendency for the enzymes to relax by HP and evolve H_2 or proceed productively by *re* of H_2 with coupled capture/reduction of N_2. The rate constant for hydride protonolysis (k_{HP}) varies by less than a factor of 2 among the three enzymes, but the rate constant for cleavage of the N≡N triple bond, the key step in which *re* of H_2 is coupled to N_2 binding/reaction (k_{re}) for Mo-nitrogenase, is ∼3-fold higher than for V-nitrogenase, and ∼10-fold higher than for Fe-nitrogenase. Thus, the differences in reactivity among the three nitrogenases result from differences in the reactivity toward N_2, rather than differences in rate constants for hydride protonolysis.

Of particular note, the finding that high-flux turnover by all three enzymes is described by eq 6 for r implies that all three nitrogenases approach the ratio, $r = H_2/N_2 \rightarrow 1$ that is exhibited by this equation at sufficiently high P_{N_2}, namely the stoichiometry of the *re/oa* mechanism, eq 1. The erroneous limiting values previously reported for V- and Fe-nitrogenases[8,13,28] (eqs 2 and 3) merely represent experimental limitations in the abilities to employ pressures of N_2 that are sufficient to approach the true limiting value. For Mo-nitrogenase, r approaches unity at $P_{N_2} \sim 50$ atm.[27] Considerably higher pressures would be needed for the other two, *not* because they have a greater tendency for $E_4(4H)$ to relax by hydride protonolysis (k_{HP}), but because they are less capable of undergoing productive conversion to $E_4(2N2H)$ – their rate constants k_{re} are less.

Origin of the Differences in Catalytic Efficiency. These high-flux studies of the three nitrogenases focus on the competing reactions of their $E_4(4H)$ Janus intermediate: "productive" *re* of H_2 with binding/reaction of N_2, rate constant, k_{re}, vs HP of a bridging hydride that relaxes the enzyme back toward E_0, rate constant, k_{HP}, Figure 3. As noted just above, examination of Table 1 shows the value of k_{HP} varies little with the identity of the enzyme. This would seem to be unsurprising, as it implies that the reactivity of an Fe–H–Fe bridging hydride with a proton on or near Fe*M*-co is largely independent of the "terminal" heterometal *M*. In contrast, the rate constant for *re* of H_2, k_{re}, is extremely sensitive to the nitrogenase form, being 3-fold smaller for V-nitrogenase than the Mo-nitrogenase and 10-fold smaller for Fe-nitrogenase. The protein environment of the active-site Fe*M*-co is known to play a significant role in reactivity, and these differences likely contribute to the differences in reactivity.[10,54−57] In addition, a direct sensitivity to the heterometal is a strong possibility, given recent X-ray[58] and theoretical reports of strong metal–metal bonding between the heterometal and the Fe ions. The reductive-elimination of H_2 implies the concomitant double-reduction of the Fe*M*-co, and this is accompanied by N_2 binding/reduction. The presence of such metal–metal bonding suggests that this process may depend on the electronic structure of the Fe*M*-co *as a whole* and that this is differentially "tuned" by the different heterometal ions. For example, a variation of k_{re} with heterometal might reflect a much greater difficulty in reducing FeFe-co through *re* of H_2 than FeMo-co and a noticeably greater difficulty in reducing FeV-co.

■ ASSOCIATED CONTENT

Supporting Information

The Supporting Information is available free of charge on the ACS Publications website at DOI: 10.1021/acs.biochem.9b00468.

Equation S1, corresponding rate constant for H_2 production for Scheme B; Figure S1, HD formation by nitrogenase; Table S1, specific activities of P_{N_2} titration, equation used in QtiPlot, and derived constants from Figure 5; Table S2, values for ratio of H_2 produced to N_2 reduced per P_{N_2}, equation used in QtiPlot, and derived rate constants from Figure 6; Table S3, values for ratio of H_2 produced to N_2 reduced per *M*Fe:Fe molar ratio, equation used in QtiPlot, and derived values from Figure 4 (PDF)

Accession Codes

nitrogenase molybdenum–iron protein alpha chain – NifD, UniProtKB P07328; nitrogenase molybdenum–iron protein beta chain – NifK, UniProtKB P07329; nitrogenase iron protein 1 – NifH, UniProtKB P00459; nitrogenase vanadium–iron protein alpha chain – VnfD, UniProtKB P16855; nitrogenase vanadium–iron protein beta chain – VnfK, UniProtKB P16856; nitrogenase vanadium–iron protein delta chain – VnfG, UniProtKB P16857; nitrogenase iron protein 2 – VnfH, UniProtKB P15335; nitrogenase iron–iron protein alpha chain – AnfD, UniProtKB P16266; nitrogenase iron–iron protein beta chain – AnfK, UniProtKB P16267; nitrogenase iron–iron protein delta chain – AnfG, UniProtKB

DOI: 10.1021/acs.biochem.9b00468
Biochemistry 2019, 58, 3293−3301

P16268; nitrogenase iron protein 3 − AnfH, UniProtKB P16269

AUTHOR INFORMATION

Corresponding Authors

*Phone: +1.435.797.3964. E-mail: lance.seefeldt@usu.edu (L.C.S.).
*Phone: +1.847.491.3104. E-mail: bmh@northwestern.edu (B.M.H.).

ORCID

Derek F. Harris: 0000-0003-4277-2976
Dmitriy A. Lukoyanov: 0000-0002-4542-1648
Hayden Kallas: 0000-0003-3882-6003
Zhi-Yong Yang: 0000-0001-8186-9450
Neil Kelleher: 0000-0002-8815-3372
Oliver Einsle: 0000-0001-8722-2893
Brian M. Hoffman: 0000-0002-3100-0746
Lance C. Seefeldt: 0000-0002-6457-9504

Funding

Support for the cell growth, protein purification, and kinetic analysis was provided by the U.S. Department of Energy, Office of Science, Basic Energy Sciences (BES) under awards to L.C.S. and D.R.D. (DE-SC0010687 and DE-SC0010834). Mass spectroscopic measurements and kinetic analyses were initiated with support from the National Science Foundation award to B.M.H. (MCB 1515981) and completed with the benefit of additional support from a U.S. Department of Energy, Office of Science, Basic Energy Sciences (BES) award to B.M.H. (DE-SC0019342). The production of V-nitrogenase was supported by Deutsche Forschungsgemeinschaft (RTG 1976 and PP 1927 to O.E.) and the European Research Council (grant 310656 to O.E.).

Notes

The authors declare no competing financial interest.

REFERENCES

(1) Raymond, J., Siefert, J. L., Staples, C. R., and Blankenship, R. E. (2004) The natural history of nitrogen fixation. *Mol. Biol. Evol. 21*, 541−554.

(2) Burris, R. H., and Roberts, G. P. (1993) Biological nitrogen fixation. *Annu. Rev. Nutr. 13*, 317−335.

(3) Gruber, N., and Galloway, J. N. (2008) An Earth-system perspective of the global nitrogen cycle. *Nature 451*, 293−296.

(4) Eady, R. R. (1996) Structure-function relationships of alternative nitrogenases. *Chem. Rev. 96*, 3013−3030.

(5) Burgess, B. K., and Lowe, D. J. (1996) Mechanism of molybdenum nitrogenase. *Chem. Rev. 96*, 2983−3012.

(6) Hu, Y., Lee, C. C., and Ribbe, M. W. (2012) Vanadium nitrogenase: A two-hit wonder? *Dalton Trans. 41*, 1118−1127.

(7) Joerger, R. D., Jacobson, M. R., Premakumar, R., Wolfinger, E. D., and Bishop, P. E. (1989) Nucleotide sequence and mutational analysis of the structural genes (*anfHDGK*) for the second alternative nitrogenase from *Azotobacter vinelandii*. *J. Bacteriol. 171*, 1075−1086.

(8) Schneider, K., and Müller, A. (2004) Iron-only nitrogenase: Exceptional catalytic, structural and spectroscopic features, in *Catalysts for Nitrogen Fixation*, pp 281−307, Springer, Dordrecht, DOI: 10.1007/978-1-4020-3611-8_11.

(9) Hales, B. J. (1990) Alternative nitrogenase. *Adv. Inorg. Biochem. 8*, 165−198.

(10) Hoffman, B. M., Lukoyanov, D., Yang, Z.-Y., Dean, D. R., and Seefeldt, L. C. (2014) Mechanism of Nitrogen Fixation by Nitrogenase: The Next Stage. *Chem. Rev. 114*, 4041−4062.

(11) Fay, A. W., Blank, M. A., Lee, C. C., Hu, Y., Hodgson, K. O., Hedman, B., and Ribbe, M. W. (2010) Characterization of isolated nitrogenase FeVco. *J. Am. Chem. Soc. 132*, 12612−12618.

(12) Krahn, E., Weiss, B., Kröckel, M., Groppe, J., Henkel, G., Cramer, S., Trautwein, A., Schneider, K., and Müller, A. (2002) The Fe-only nitrogenase from *Rhodobacter capsulatus*: identification of the cofactor, an unusual, high-nuclearity iron-sulfur cluster, by Fe K-edge EXAFS and ^{57}Fe Mössbauer spectroscopy. *JBIC, J. Biol. Inorg. Chem. 7*, 37−45.

(13) Harris, D. F., Lukoyanov, D. A., Shaw, S., Compton, P., Tokmina-Lukaszewska, M., Bothner, B., Kelleher, N., Dean, D. R., Hoffman, B. M., and Seefeldt, L. C. (2018) Mechanism of N_2 reduction catalyzed by Fe-nitrogenase involves reductive elimination of H_2. *Biochemistry 57*, 701−710.

(14) Sippel, D., and Einsle, O. (2017) The structure of vanadium nitrogenase reveals an unusual bridging ligand. *Nat. Chem. Biol. 13*, 956−960.

(15) Georgiadis, M. M., Komiya, H., Chakrabarti, P., Woo, D., Kornuc, J. J., and Rees, D. C. (1992) Crystallographic structure of the nitrogenase iron protein from *Azotobacter vinelandii*. *Science 257*, 1653−1659.

(16) Rohde, M., Trncik, C., Sippel, D., Gerhardt, S., and Einsle, O. (2018) Crystal structure of VnfH, the iron protein component of vanadium nitrogenase. *JBIC, J. Biol. Inorg. Chem. 23*, 1049−1056.

(17) Spatzal, T., Aksoyoglu, M., Zhang, L., Andrade, S. L. A., Schleicher, E., Weber, S., Rees, D. C., and Einsle, O. (2011) Evidence for interstitial carbon in nitrogenase FeMo cofactor. *Science 334*, 940−940.

(18) Peters, J. W., Fisher, K., Newton, W. E., and Dean, D. R. (1995) Involvement of the P-cluster in intramolecular electron transfer within the nitrogenase MoFe protein. *J. Biol. Chem. 270*, 27007−27013.

(19) Chan, J. M., Christiansen, J., Dean, D. R., and Seefeldt, L. C. (1999) Spectroscopic evidence for changes in the redox state of the nitrogenase P-cluster during turnover. *Biochemistry 38*, 5779−5785.

(20) Danyal, K., Dean, D. R., Hoffman, B. M., and Seefeldt, L. C. (2011) Electron transfer within nitrogenase: evidence for a deficit-spending mechanism. *Biochemistry 50*, 9255−9263.

(21) Thorneley, R. N. F., and Lowe, D. J. (1985) Kinetics and mechanism of the nitrogenase enzyme, in *Molybdenum Enzymes* (Spiro, T. G., Ed.), pp 221−284, Wiley-Interscience Publications, New York.

(22) Lukoyanov, D., Yang, Z.-Y., Khadka, N., Dean, D. R., Seefeldt, L. C., and Hoffman, B. M. (2015) Identification of a key catalytic intermediate demonstrates that nitrogenase is activated by the reversible exchange of N_2 for H_2. *J. Am. Chem. Soc. 137*, 3610−3615.

(23) Lukoyanov, D., Khadka, N., Yang, Z.-Y., Dean, D. R., Seefeldt, L. C., and Hoffman, B. M. (2016) Reductive elimination of H_2 activates nitrogenase to reduce the N≡N triple bond: characterization of the E_4(4H) Janus intermediate in wild-type enzyme. *J. Am. Chem. Soc. 138*, 10674−10683.

(24) Lukoyanov, D., Khadka, N., Yang, Z.-Y., Dean, D. R., Seefeldt, L. C., and Hoffman, B. M. (2016) Reversible photoinduced reductive elimination of H_2 from the nitrogenase dihydride state, the E_4(4H) Janus intermediate. *J. Am. Chem. Soc. 138*, 1320−1327.

(25) Raugei, S., Seefeldt, L. C., and Hoffman, B. M. (2018) Critical computational analysis illuminates the reductive-elimination mechanism that activates nitrogenase for N_2 reduction. *Proc. Natl. Acad. Sci. U. S. A. 115*, E10521−E10530.

(26) Rohde, M., Sippel, D., Trncik, C., Andrade, S. L. A., and Einsle, O. (2018) The critical E_4 state of nitrogenase catalysis. *Biochemistry 57*, 5497−5504.

(27) Simpson, F. B., and Burris, R. H. (1984) A nitrogen pressure of 50 atm does not prevent evolution of hydrogen by nitrogenase. *Science 224*, 1095−1097.

(28) Eady, R. R., Robson, R. L., Richardson, T. H., Miller, R. W., and Hawkins, M. (1987) The vanadium nitrogenase of *Azotobacter chroococcum*. Purification and properties of the VFe protein. *Biochem. J. 244*, 197−207.

DOI: 10.1021/acs.biochem.9b00468
Biochemistry 2019, 58, 3293−3301

(29) Harris, D. F., Yang, Z.-Y., Dean, D. R., Seefeldt, L. C., and Hoffman, B. M. (2018) Kinetic understanding of N_2 reduction versus H_2 evolution at the E_4(4H) Janus state in the three nitrogenases. *Biochemistry 57*, 5706−5714.
(30) Christiansen, J., Goodwin, P. J., Lanzilotta, W. N., Seefeldt, L. C., and Dean, D. R. (1998) Catalytic and biophysical properties of a nitrogenase apo-MoFe protein produced by an *nifB*-deletion mutant of *Azotobacter vinelandii*. *Biochemistry 37*, 12611−12623.
(31) Burgess, B. K., Jacobs, D. B., and Stiefel, E. I. (1980) Large-scale purification of high activity *Azotobacter vinelandii* nitrogenase. *Biochim. Biophys. Acta 614*, 196−209.
(32) Peters, J. W., Fisher, K., and Dean, D. R. (1994) Identification of a nitrogenase protein-protein interaction site defined by residues 59 through 67 within the *Azotobacter vinelandii* Fe protein. *J. Biol. Chem. 269*, 28076−28083.
(33) Sippel, D., Schlesier, J., Rohde, M., Trncik, C., Decamps, L., Djurdjevic, I., Spatzal, T., Andrade, S. L. A., and Einsle, O. (2017) Production and isolation of vanadium nitrogenase from *Azotobacter vinelandii* by molybdenum depletion. *JBIC, J. Biol. Inorg. Chem. 22*, 161−168.
(34) Corbin, J. L. (1984) Liquid chromatographic-fluorescence determination of ammonia from nitrogenase reactions: A 2-min assay. *Appl. Environ. Microbiol. 47*, 1027−1030.
(35) Barney, B. M., Igarashi, R. Y., Dos Santos, P. C., Dean, D. R., and Seefeldt, L. C. (2004) Substrate interaction at an iron-sulfur face of the FeMo-cofactor during nitrogenase catalysis. *J. Biol. Chem. 279*, 53621−53624.
(36) Guth, J. H., and Burris, R. H. (1983) Inhibition of nitrogenase-catalyzed ammonia formation by hydrogen. *Biochemistry 22*, 5111−5122.
(37) Burgess, B. K., Wherland, S., Newton, W. E., and Stiefel, E. I. (1981) Nitrogenase reactivity: insight into the nitrogen-fixing process through hydrogen-inhibition and HD-forming reactions. *Biochemistry 20*, 5140−5146.
(38) Seefeldt, L. C., Hoffman, B. M., and Dean, D. R. (2009) Mechanism of Mo-dependent nitrogenase. *Annu. Rev. Biochem. 78*, 701−722.
(39) Thorneley, R. N. F., and Lowe, D. J. (1983) Nitrogenase of *Klebsiella pneumoniae*. Kinetics of the dissociation of oxidized iron protein from molybdenum-iron protein: identification of the rate-limiting step for substrate reduction. *Biochem. J. 215*, 393−403.
(40) Thorneley, R. N., and Lowe, D. J. (1984) The mechanism of *Klebsiella pneumoniae* nitrogenase action. Pre-steady-state kinetics of an enzyme-bound intermediate in N_2 reduction and of NH_3 formation. *Biochem. J. 224*, 887−894.
(41) Lowe, D. J., and Thorneley, R. N. (1984) The mechanism of *Klebsiella pneumoniae* nitrogenase action. The determination of rate constants required for the simulation of the kinetics of N_2 reduction and H_2 evolution. *Biochem. J. 224*, 895−901.
(42) Lowe, D. J., and Thorneley, R. N. (1984) The mechanism of *Klebsiella pneumoniae* nitrogenase action. Pre-steady-state kinetics of H_2 formation. *Biochem. J. 224*, 877−886.
(43) Peters, J. W., Stowell, M. H. B., Soltis, S. M., Finnegan, M. G., Johnson, M. K., and Rees, D. C. (1997) Redox-Dependent structural changes in the nitrogenase P-cluster. *Biochemistry 36*, 1181−1187.
(44) Schindelin, H., Kisker, C., Schlessman, J. L., Howard, J. B., and Rees, D. C. (1997) Structure of ADP·AlF_4^--stabilized nitrogenase complex and its implications for signal transduction. *Nature 387*, 370−376.
(45) Tezcan, F. A., Kaiser, J. T., Mustafi, D., Walton, M. Y., Howard, J. B., and Rees, D. C. (2005) Nitrogenase complexes: multiple docking sites for a nucleotide switch protein. *Science 309*, 1377−1380.
(46) Einsle, O., Tezcan, F. A., Andrade, S. L. A., Schmid, B., Yoshida, M., Howard, J. B., and Rees, D. C. (2002) Nitrogenase MoFe-protein at 1.16 Å resolution: a central ligand in the FeMo-cofactor. *Science 297*, 1696−1700.
(47) Sarma, R., Barney, B. M., Keable, S., Dean, D. R., Seefeldt, L. C., and Peters, J. W. (2010) Insights into substrate binding at FeMo-cofactor in nitrogenase from the structure of an α-70Ile MoFe protein variant. *J. Inorg. Biochem. 104*, 385−389.
(48) Spatzal, T., Perez, K. A., Einsle, O., Howard, J. B., and Rees, D. C. (2014) Ligand binding to the FeMo-cofactor: structures of CO-bound and reactivated nitrogenase. *Science 345*, 1620−1623.
(49) Sørlie, M., Christiansen, J., Lemon, B. J., Peters, J. W., Dean, D. R., and Hales, B. J. (2001) Mechanistic features and structure of the nitrogenase α-Gln195 MoFe protein. *Biochemistry 40*, 1540−1549.
(50) Tittsworth, R. C., and Hales, B. J. (1996) Oxidative titration of the nitrogenase VFe protein from *Azotobacter vinelandii*: an example of redox-gated electron flow. *Biochemistry 35*, 479−487.
(51) Blanchard, C. Z., and Hales, B. J. (1996) Isolation of two forms of the nitrogenase VFe protein from *Azotobacter vinelandii*. *Biochemistry 35*, 472−478.
(52) Hales, B. J., Case, E. E., Morningstar, J. E., Dzeda, M. F., and Mauterer, L. A. (1986) Isolation of a new vanadium-containing nitrogenase from *Azotobacter vinelandii*. *Biochemistry 25*, 7251−7255.
(53) Sippel, D., Rohde, M., Netzer, J., Trncik, C., Gies, J., Grunau, K., Djurdjevic, I., Decamps, L., Andrade, S. L. A., and Einsle, O. (2018) A bound reaction intermediate sheds light on the mechanism of nitrogenase. *Science 359*, 1484−1489.
(54) Yang, Z.-Y., Moure, V. R., Dean, D. R., and Seefeldt, L. C. (2012) Carbon dioxide reduction to methane and coupling with acetylene to form propylene catalyzed by remodeled nitrogenase. *Proc. Natl. Acad. Sci. U. S. A. 109*, 19644−19648.
(55) Rebelein, J. G., Lee, C. C., Newcomb, M., Hu, Y., and Ribbe, M. W. (2018) Characterization of an M-cluster-substituted nitrogenase VFe protein. *mBio 9*, E00310−E00318.
(56) Seefeldt, L. C., Yang, Z.-Y., Duval, S., and Dean, D. R. (2013) Nitrogenase reduction of carbon-containing compounds. *Biochim. Biophys. Acta, Bioenerg. 1827*, 1102−1111.
(57) Khadka, N., Dean, D. R., Smith, D., Hoffman, B. M., Raugei, S., and Seefeldt, L. C. (2016) CO_2 Reduction catalyzed by nitrogenase: pathways to formate, carbon monoxide, and methane. *Inorg. Chem. 55*, 8321−8330.
(58) Rees, J. A., Bjornsson, R., Kowalska, J. K., Lima, F. A., Schlesier, J., Sippel, D., Weyhermüller, T., Einsle, O., Kovacs, J. A., and DeBeer, S. (2017) Comparative electronic structures of nitrogenase FeMoco and FeVco. *Dalton Trans 46*, 2445−2455.

DOI: 10.1021/acs.biochem.9b00468
Biochemistry 2019, 58, 3293−3301